

Applications of DFT to nanoclusters

Hannu Häkkinen

FYSM540

8.12.2008

University of Jyväskylä

Nanoscience Center

Departments of Physics and Chemistry

All things are made of atoms...

- ...in order for physical theory to be of any use, we must know where the atoms are located...
- ... in order to understand chemistry, we must know what atoms are present...
- ... if all the scientific knowledge were to be destroyed, and only one sentence passed on to the next generation of creatures, what statement would contain the most information in the fewest words?

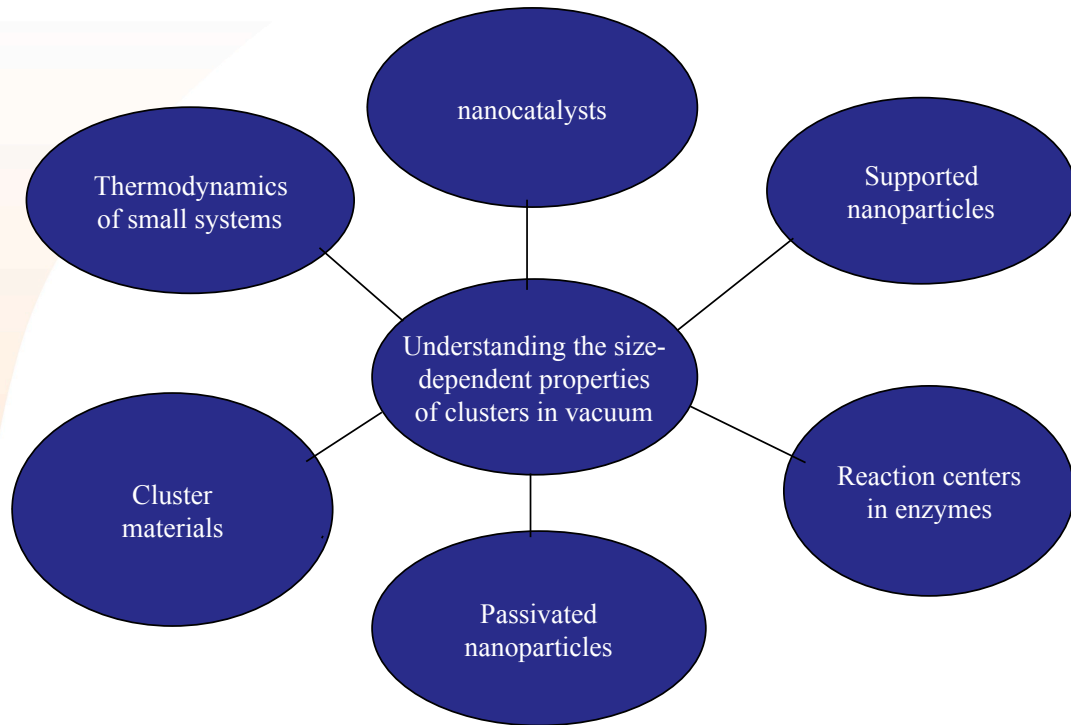
I believe it is ... **that all things are made of atoms**



Feynman's Preface

These are the lectures in physics that I gave last year and the year before to the freshman and sophomore classes at Caltech. The lectures are, of course, not verbatim—they have been edited, sometimes extensively and sometimes less so.

Cluster science – at the heart of "Nano" !



Contents

- Manufacturing of nanoclusters
- Cluster stability: atomic and electronic shells
- Experiment vs. theory: Na clusters from 4 to 350 atoms
- Thermodynamic properties
- Chemical and catalytic properties (example: gold)
- Ligand-protected Au clusters

Some literature

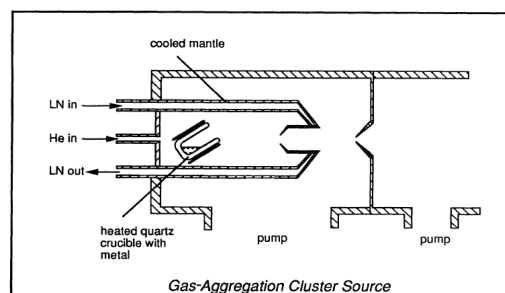
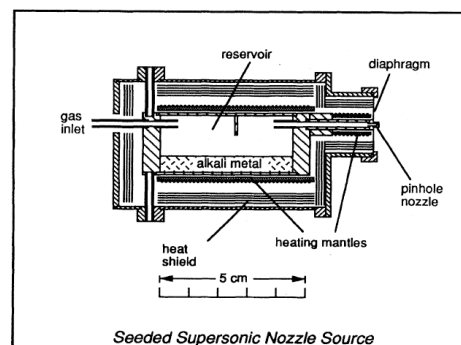
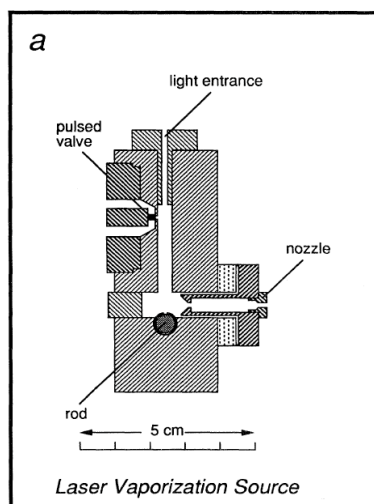
- R. L. Johnston, Atomic and Molecular Clusters, Taylor & Francis (2002).
- W. A. de Heer, The physics of simple metal clusters: Experimental aspects and simple models, Rev. Mod. Phys **65**, 611 (1993).
- M. Brack, The physics of simple metal clusters: Self-consistent jellium model and semiclassical approaches, Rev. Mod. Phys. **65**, 677 (1993).
- F. Baletto, R. Ferrando, Structural properties of nanoclusters: Energetic, thermodynamic, and kinetic effects, Rev. Mod. Phys. **77**, 371 (2005).
- T. P. Martin, Shells of atoms, Phys. Rep. **273**, 199 (1996).

Making nanoclusters

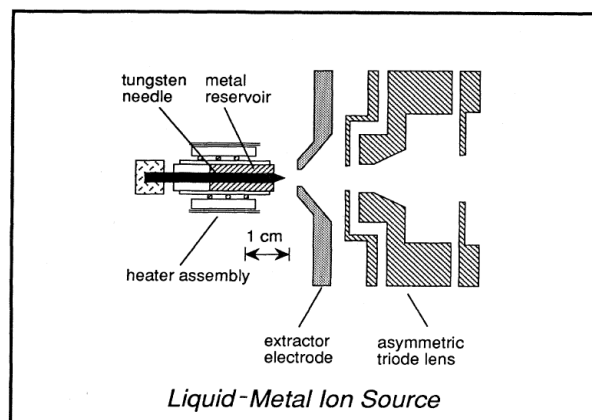
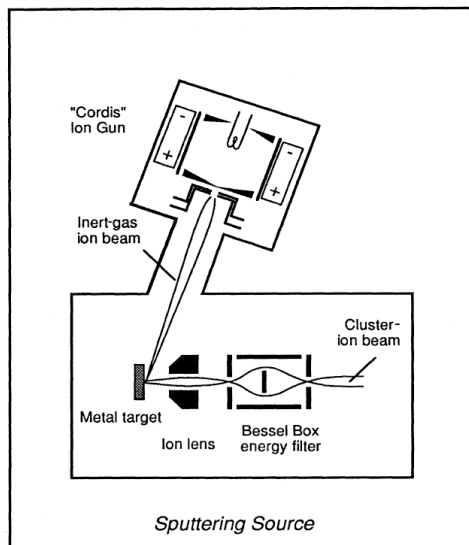
Cluster sources

- Seeded supersonic nozzle source
- Gas-aggregation source
- Laser vaporization source
- Sputtering source
- Liquid-metal ion source

Cluster sources



Cluster sources



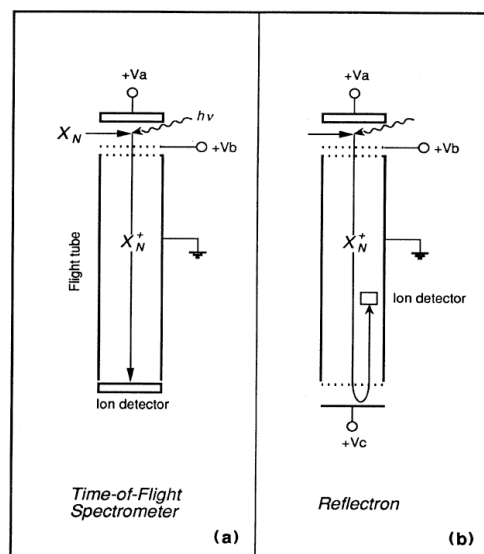
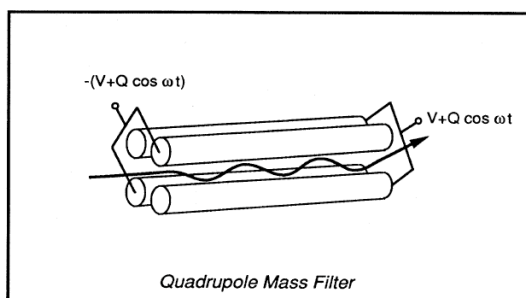
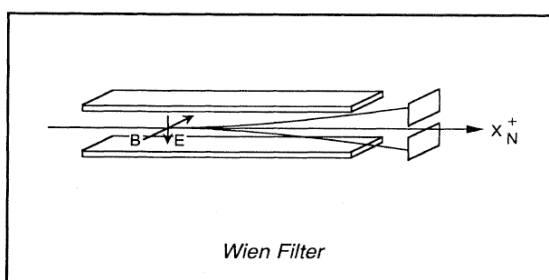
Cluster sources – overview

- Seeded supersonic nozzle source: intense continuous beams, low-boiling-point materials, evaporative cooling -> structured mass spectra (magic stabilities visible), temperature not well controlled
- Gas-aggregation cluster source: efficient for production of large clusters (up to 20 000+), low intensity, low-to-medium boiling point materials (< 2000 K), low cluster temperature (< 100 K)
- Laser vaporization source: pulsed beams from any material, cluster temperature near the source temperature
- Sputtering source: energetic heavy inert-gas ion sputtering beam (Kr⁺, Xe⁺, 10 – 20 keV) -> continuous beam of singly ionized (hot) clusters, cooling by evaporation
- Liquid-metal ion source: singly and multiply ionized (hot) clusters of low-melting-point metals

Analysis techniques

- Wien filter
- Quadrupole mass filter
- Time-of-flight mass spectrometry
- Ion cyclotron resonance mass spectrometry in ion trap
- Molecular-beam mobility analysis
- Electron diffraction in ion trap (structure factor)
- Photoelectron spectroscopy

Cluster mass analysis

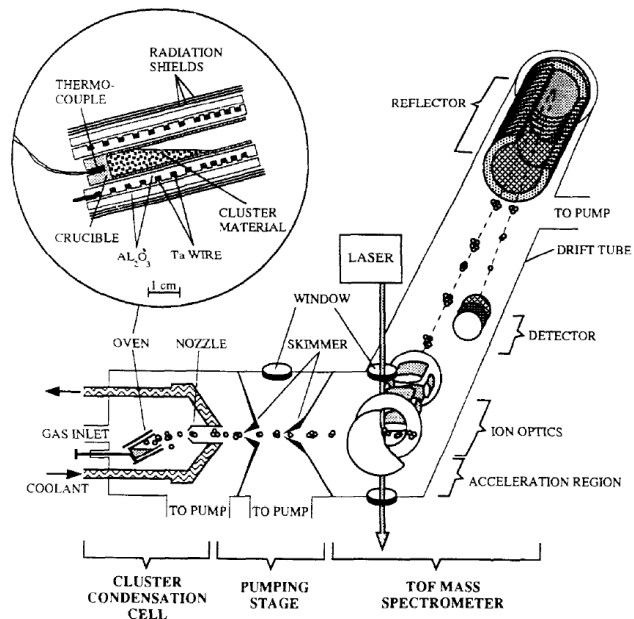


Example of a full setup

Gas-aggregation source

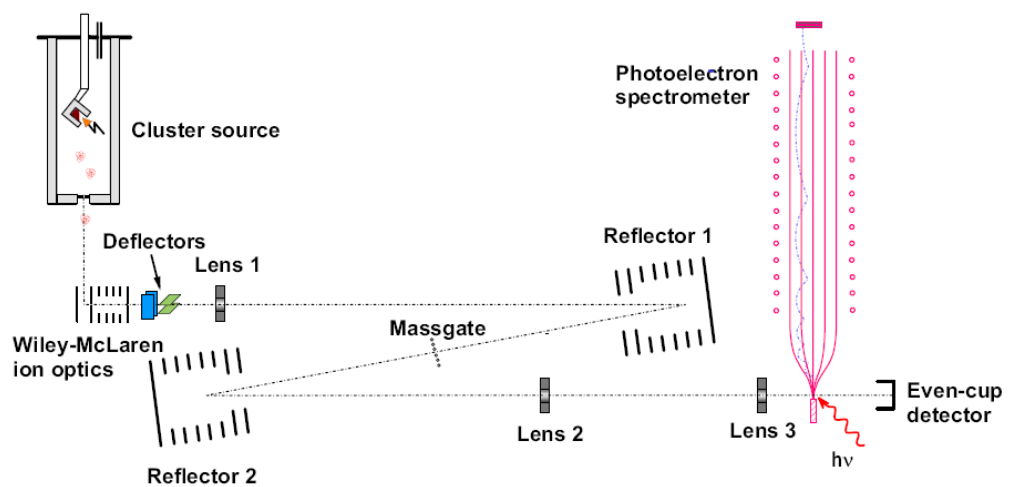
Photoionization by laser

Time-of-flight mass analysis



Martin, Phys. Rep. 273, 199 (1996)

Photoelectron spectroscopy



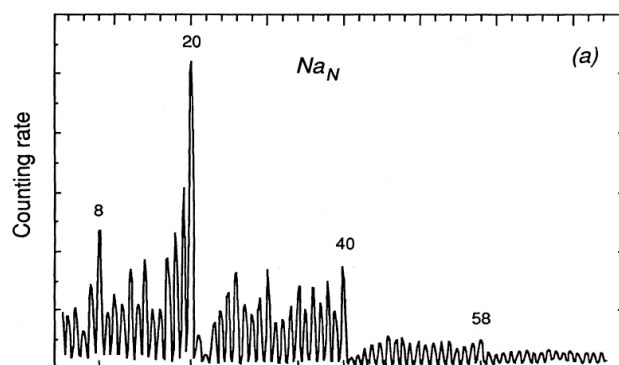
O. Kostko, PhD Thesis Freiburg 2007

Cluster stability: atomic and electronic shells

Cluster stability – "magic numbers"

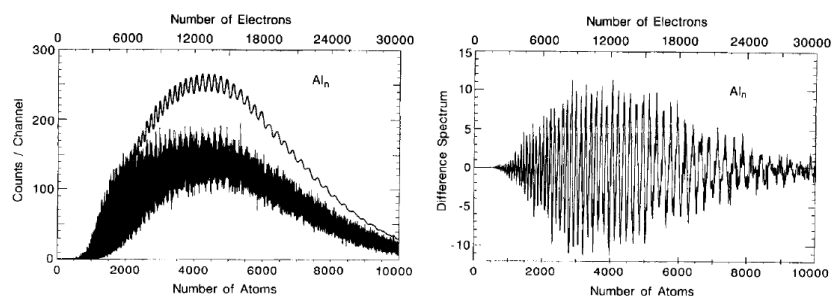
Sodium

Knight et al, Phys. Rev. Lett.
52, 2141 (1984)



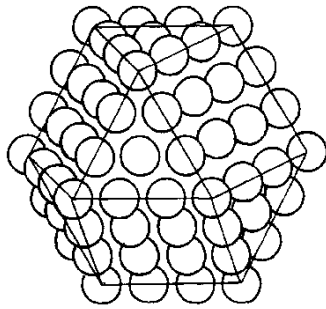
Aluminium

Martin, Phys. Rep.
273, 199 (1996)

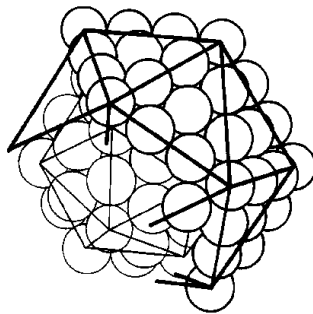


Cluster stability – atomic shells

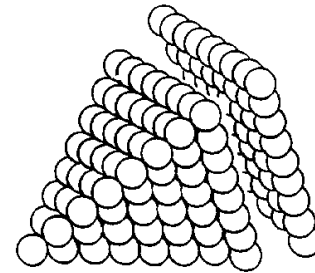
Cuboctahedron (fcc)



Icosahedron



T.P. Martin
Physics Reports
273, 199 (1996)



Tetrahedron (fcc)

QUANTUM-SIZE EFFECTS (QSE) IN METALLIC NANOPARTICLES ?

Free-electron model of metal : density of electron states $D(\epsilon) \propto \sqrt{\epsilon}$

Mean spacing of electron levels at the Fermi level ϵ_F :

$$\delta(\epsilon_F) = 1 / D(\epsilon_F) \sim 2 \epsilon_F / 3 N z \quad (N = \text{number of atoms}, z = \text{valence number})$$

QSE visible when $\delta > kT$ ($kT = 0.025$ eV at 300 K)

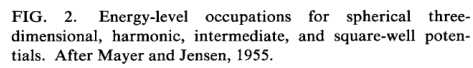
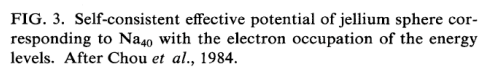
Au, $\epsilon_F = 5.5$ eV, $z = 1 \rightarrow N < 150$ atoms \rightarrow diameter < 1.7 nm

Na, $\epsilon_F = 3.2$ eV, $z = 1 \rightarrow N < 85$ atoms \rightarrow diameter < 1.4 nm

(in practice: symmetry \rightarrow electron shells may increase the gaps close to ϵ_F
 \rightarrow One may observe QSE up to several hundred atoms)

QSE \rightarrow stabilization of the nanoparticle structure by electronic effects
 \rightarrow opening of the energy gap at the Fermi level (HOMO-LUMO gap)
 \rightarrow "metallic" \rightarrow "semiconductor" behaviour

FIG. 3. Self-consistent effective potential corresponding to Na_{40} with the electronic levels. After Chou *et al.*, 1984.



- Single-particle Hamiltonian

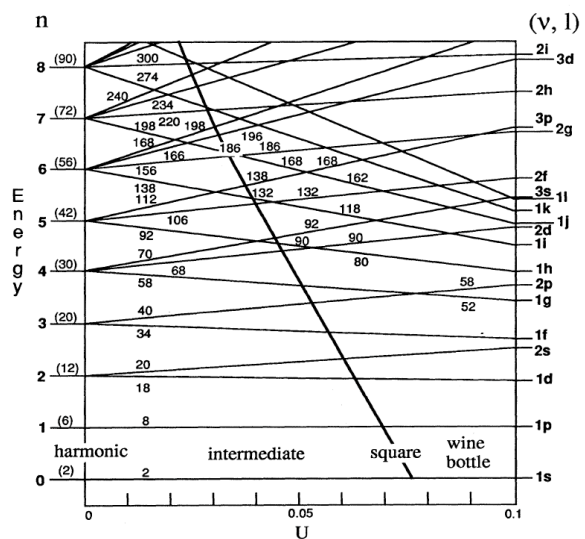
$$H = \frac{\mathbf{p}^2}{2m} + \frac{m\omega_0^2 \mathbf{q}^2}{2} - U$$

$$R_0 = r_s N^{1/3} \quad \hbar\omega$$
- Eigenvalue spectrum

$$E_n = \hbar\omega_0 \left\{ \left(n + \frac{3}{2} \right) - \right.$$

$$H = \frac{\mathbf{p}^2}{2m} + \frac{m\omega_0^2 \mathbf{q}^2}{2} - U\hbar\omega_0[l^2 - n(n+3)/6]$$

$$E_n = h\omega_0 \left\{ \left(n + \frac{3}{2} \right) - U[l^2 - n(n+3)/6] \right\}$$



Electron shells - Effect of deformations

- Clemenger (1985) <- Nilsson (nuclear physics, 1955 !) model:
for a fixed volume, the cluster shape adjusts to minimize the total energy

- Deformation → cluster radii R_x, R_y, R_z → tri-axial oscillator

$$E(n_x, n_y, n_z) = \hbar \omega_0 \left[(n_x + \frac{1}{2}) \frac{R_0}{R_x} + (n_y + \frac{1}{2}) \frac{R_0}{R_y} + (n_z + \frac{1}{2}) \frac{R_0}{R_z} \right]$$

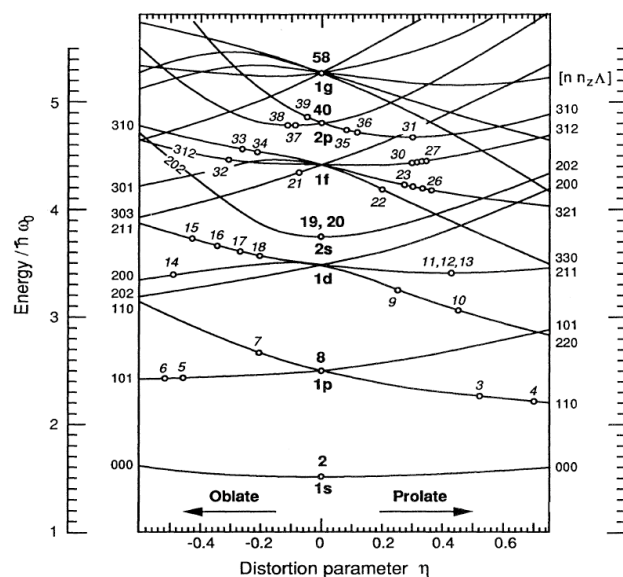
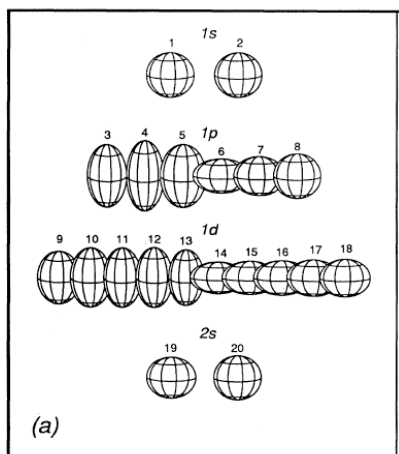
- Spheroid ($R_x = R_y$), distortion parameter

$$\eta = 2 \frac{R_z - R_x}{R_z + R_x}$$

- Total energy for spheroids

$$E_{\text{tot}}(\eta, N) = \frac{3}{4} \sum E(\eta, n_x, n_y, n_z)$$

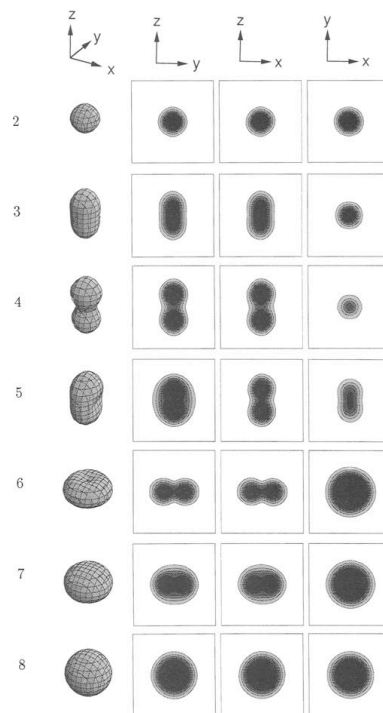
Clemenger – Nilsson diagram



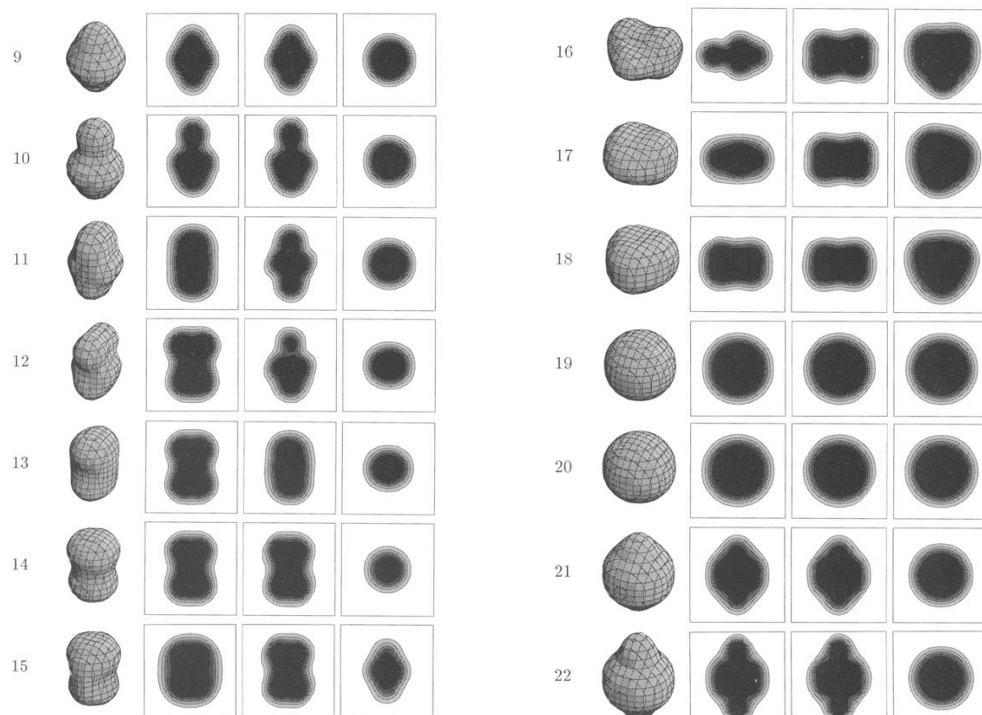
Electron-gas clusters: The "ultimate" jellium model

Koskinen, Lipas, Manninen, Z Phys D 35, 285 (95)

- neutralizing, deformable positive background charge \rightarrow no Coulomb energy
 \rightarrow total energy is a sum of KS kinetic
 + xc energy only



Jellium clusters 9 - 22



Cluster stability – electron shells

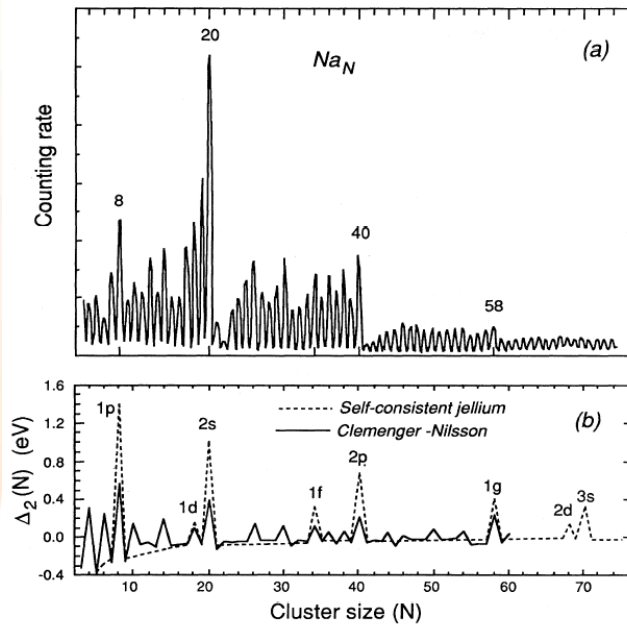
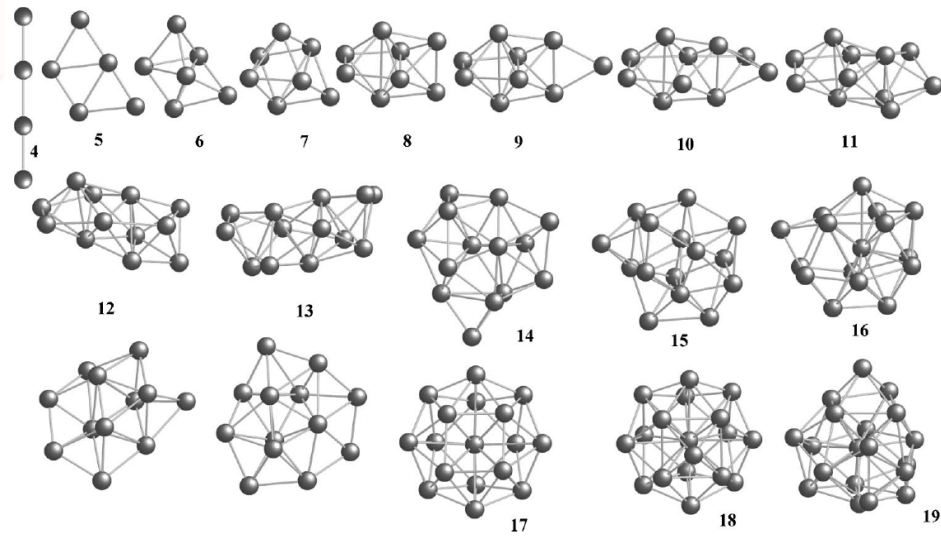


FIG. 1. Sodium cluster abundance spectrum: (a) experimental (after Knight *et al.*, 1984); (b) dashed line, using Woods-Saxon potential (after Knight *et al.*, 1984); solid line, using the ellipsoidal shell (Clemenger-Nilsson) model (after de Heer, Knight, Chou, and Cohen, 1987).

W.A. deHeer
Rev. Mod. Phys
65, 611 (1993)

Experiment vs. theory: Na clusters from 4 to 350 atoms

Na cluster anions I : optimised structures at T=0 from density functional theory (DFT)



Moseler, Huber, Häkkinen, Landman, Wrigge, Hoffman, von Issendorff, PRB **68**, 165413 (2003)

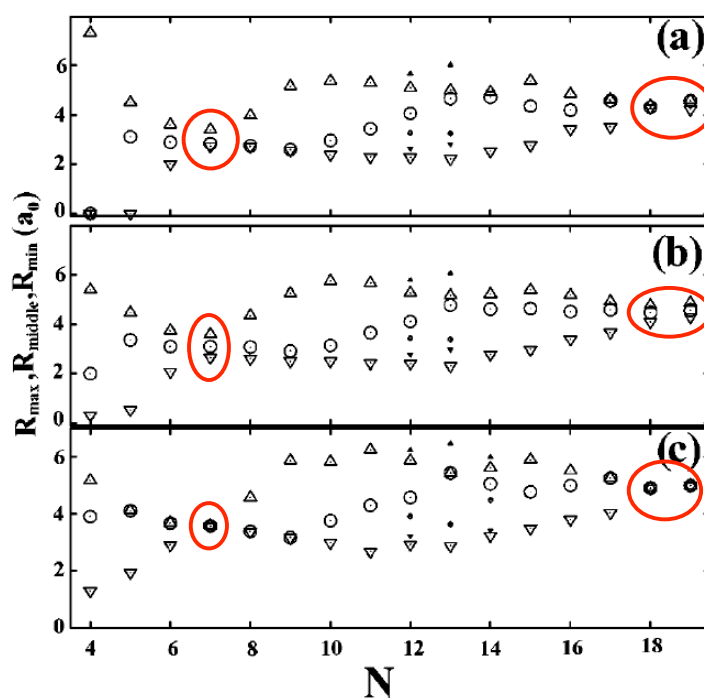
Cluster shapes from “universal jellium model”

Na cluster anions II : Cluster shapes from DFT

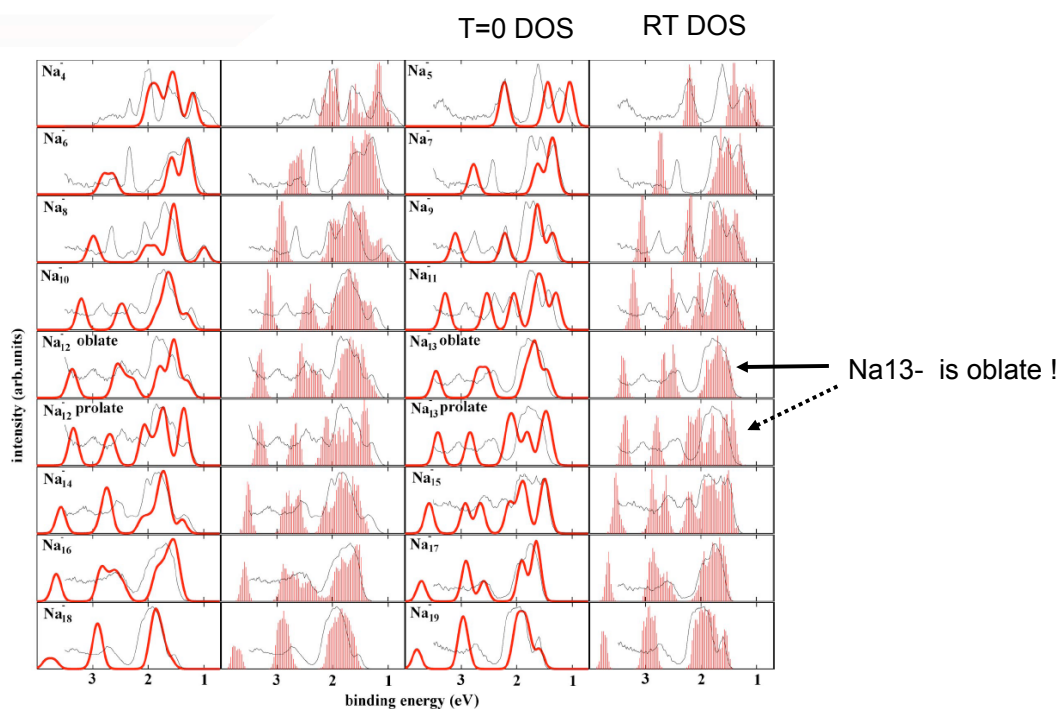
Cluster radii from GS (T=0)

Radii from RT DFT-MD

Radii from jellium model
Koskinen, Lipas, Manninen
Z. Phys. D 35, 285 (1995)



Na cluster anions III : Photoelectron spectroscopy vs. electron density of states



Na cluster anions IV : Photoelectron spectroscopy vs. electron density of states

55 → 147 → 309:

Icosahedral growth
via overlayers

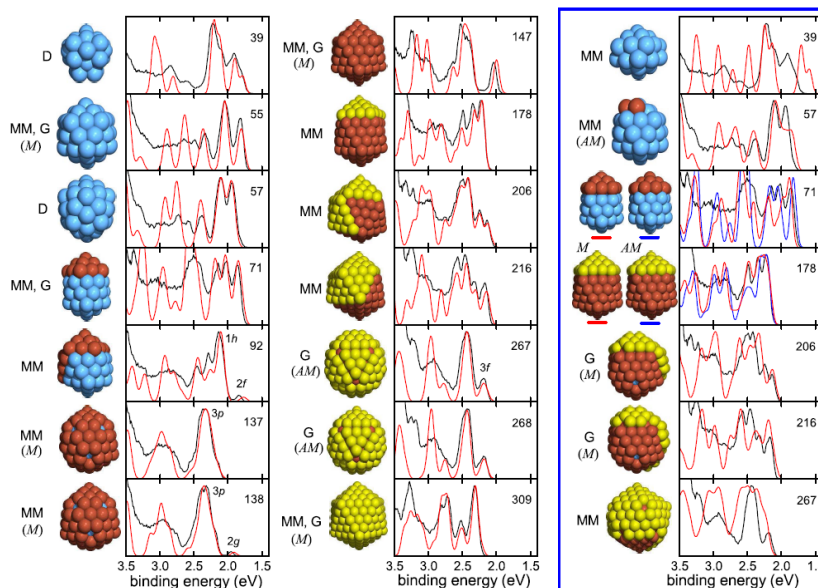


FIG. 2 (color online). Comparison of photoelectron spectra (black lines) to calculated electron densities of states (colored or shaded lines). The Kohn-Sham levels as obtained by DFT have been broadened by 70 meV width Gaussians and shifted as to reproduce the calculated electron affinity. The structures used in the calculations are indicated (left and center column: assigned ground state structures; right column: wrong structure candidates). The letters give the origin of the structures (MM: ground state structure for Murrell-Mottram potential [26], G: ground state for Gupta potential [26], D: ground state only within DFT) and indicate the structural motif of closed and open shell icosahedral structures (M/AM: Mackay/anti-Mackay overlayer [29]).

Kostko, Huber, Moseler,
Issendorff, PRL **98**,
043401 (2007)

Thermodynamic properties

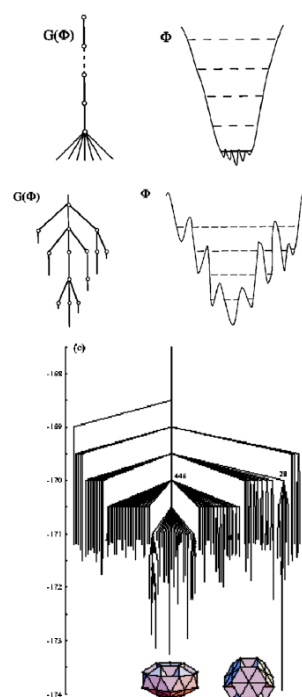
Thermodynamic properties - general

- Thermodynamics of small systems complicated and not always well defined !
- Experimental concerns: formation of clusters depends on source conditions, sometimes driven by thermodynamics, sometimes kinetics
- Nanoclusters exhibit a rich palette of thermodynamic phenomena: size-dependent melting, surface pre-melting, solid-solid structural transitions, freezing transitions, coalescence phenomena...
- Sometimes surprises in store: "non-melting clusters" (melting point appears to be higher than in bulk, e.g. Sn \leftarrow bonding different in clusters)
- Bi-stability of "phases"
- Experimentally the best studied cluster melting problem: Na clusters, work by Haberland group (original exp: Nature **393**, 238 (1998) + many later papers)
- Computational challenge: sampling of the phase-space
- Good review: Baletto, Ferrando, Rev. Mod. Phys. **77**, 371 (2005)

Global optimisation and potential energy surfaces

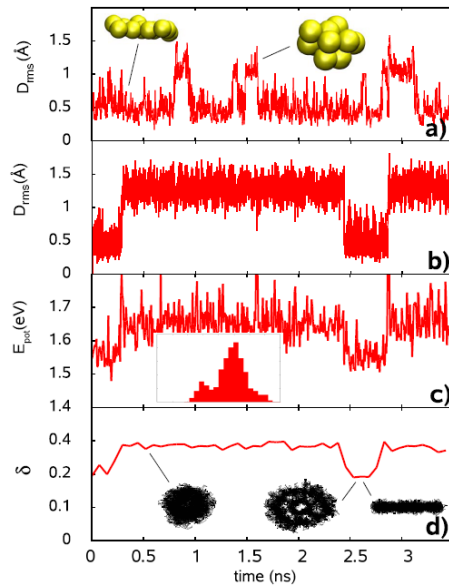
- Generally: finding **the** global optimal geometry for a given cluster size is a highly non-trivial problem
- A well-known example: 38-atom Lennard-Jones cluster has a narrow funnel for the global TO ground-state, but a wide funnel for icosahedral local minima
- A useful website for global minima: Cambridge Cluster Database www.wales.ch.cam.ac.uk/CCD.html

FIG. 11. (Color in online edition) Disconnectivity diagrams: Top panel, schematic of a single-minimum potential-energy surface (PES) with weak noise; center panel, a single-funnel PES. The disconnectivity diagrams of these two panels show at which energetic level the different local minima of a PES can be considered connected. Adapted from Becker and Karplus, 1997. The lowest panel gives the disconnectivity diagram for the complete double-funnel PES of the Lennard-Jones cluster of size 38. Figure courtesy of Jonathan Doye.

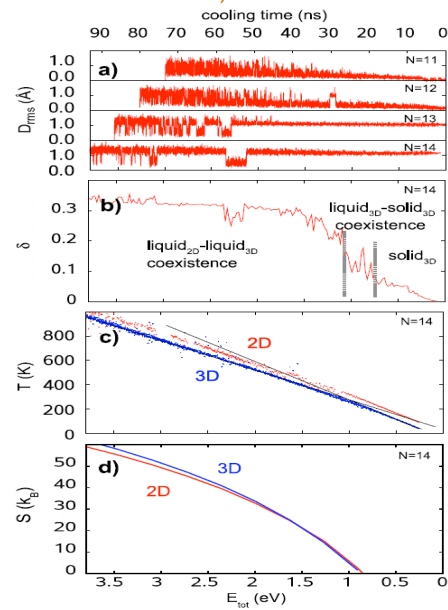


Dynamics of gold clusters from DFT-TB

MD of Au11- at 750 K:
co-existence of 2D/3D liquid



Supercooling to "wrong" dimensionality
(experimental time scale of cooling:
0.1 to 10 microseconds)



Koskinen et al, PRL 98, 015701 (2007)
Video in EPAPS

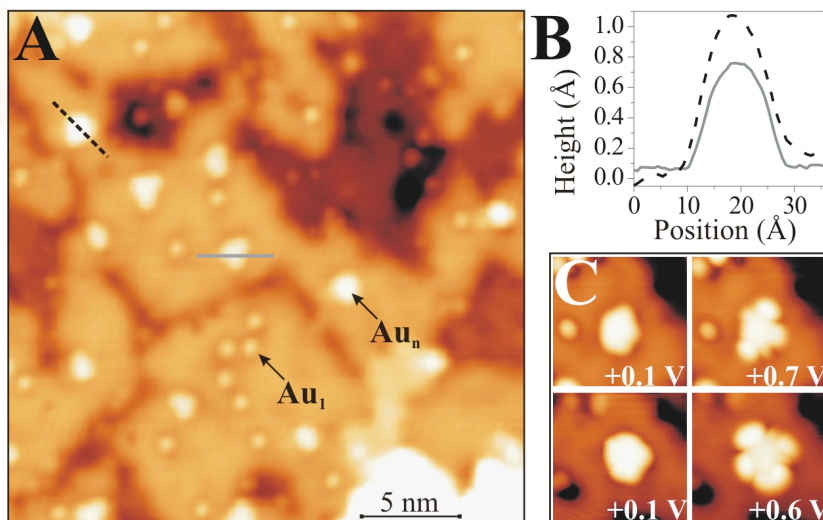
Molecular dynamics of Au14- at 750 K

Chemical and catalytic properties of gold clusters

- Bulk gold inert
- Finely dispersed gold (as nanoparticles) catalytically active, for review see eg. Haruta, Catal. Today **36**, 153 (1997)
- Oxide-supported size-selected clusters catalyze CO oxidation (Yoon, Häkkinen, Landman, Wörz, Antonietti, Abbet, Judai, Heiz, Science **307**, 403 (2005))
- Active site / charge state under debate
- Known for long: gold atom chemically active in many oxidation states (rich complex chemistry)
- Gas-phase reactivity with O₂: anionic gold needed, highly size-dependent reactivity
- Reactivity associated with electron transfer to O₂ π^* orbital

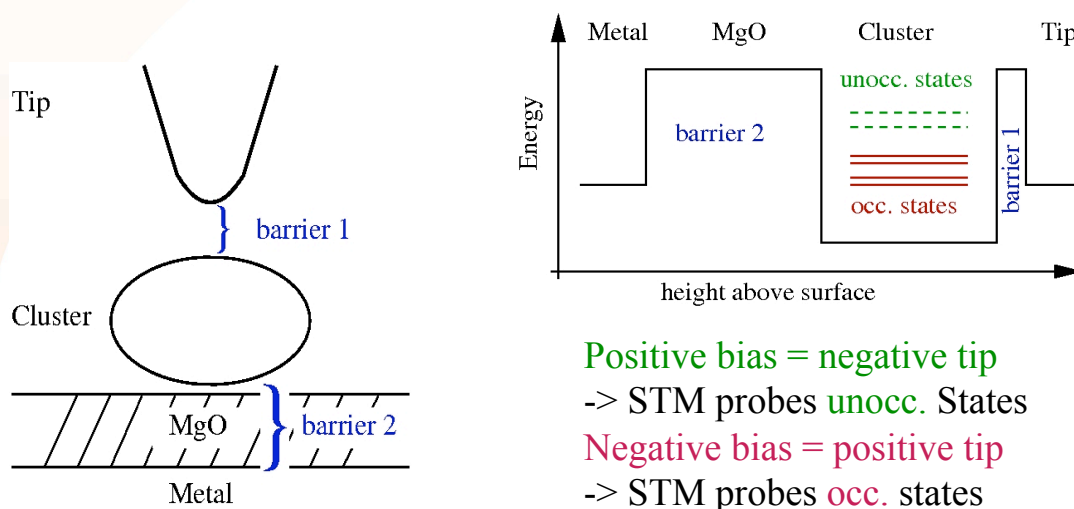
Flat Au clusters on thin MgO films

Direct experimental observations of Au clusters with STM on thin (2-3 ML) MgO films on Ag



Lin, Nilius, Freund, Walter, Frondelius, Honkala, Häkkinen, <http://arxiv.org/abs/0811.3812>

Working model

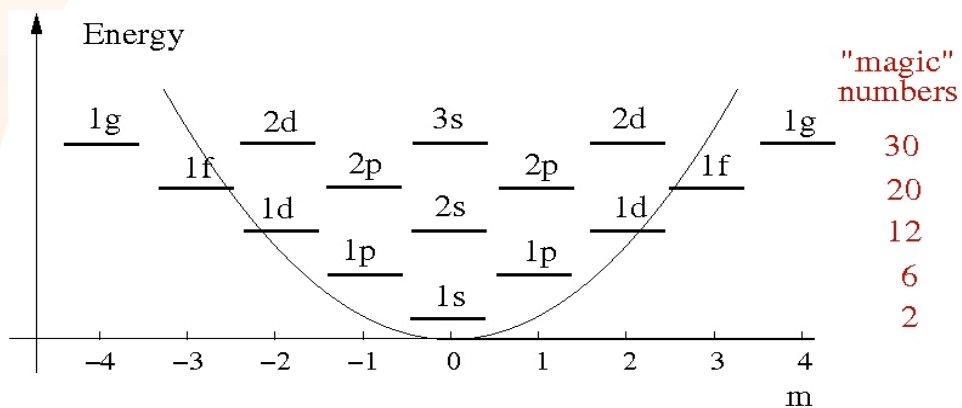


Tersoff-Hamann approximation: STM probes local DOS

Flat structure: 2D Harmonic Oscillator model

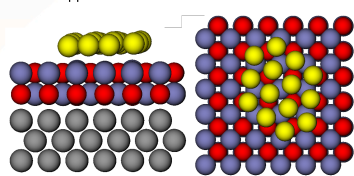


Free electrons of
monovalent Gold

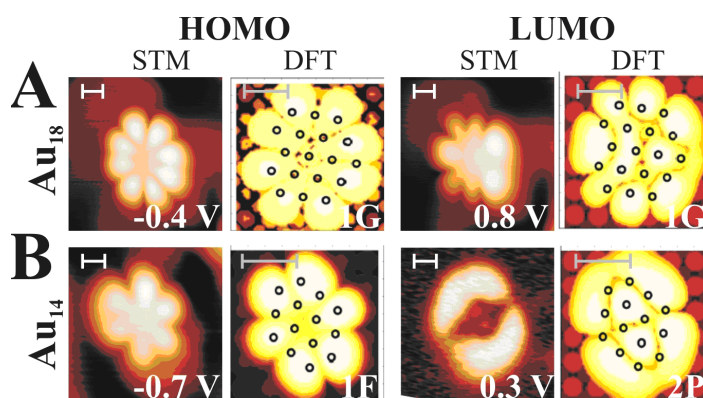
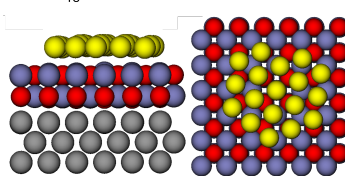


Flat Au clusters on MgO(2L)/Ag

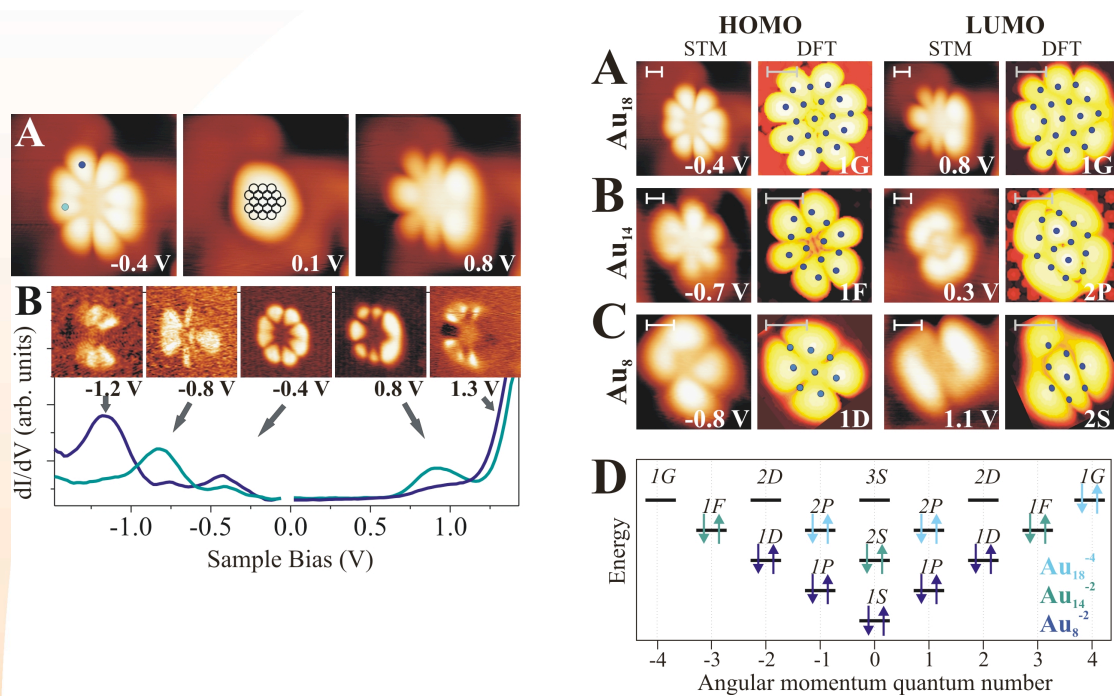
a) Au₁₄/MgO/Ag



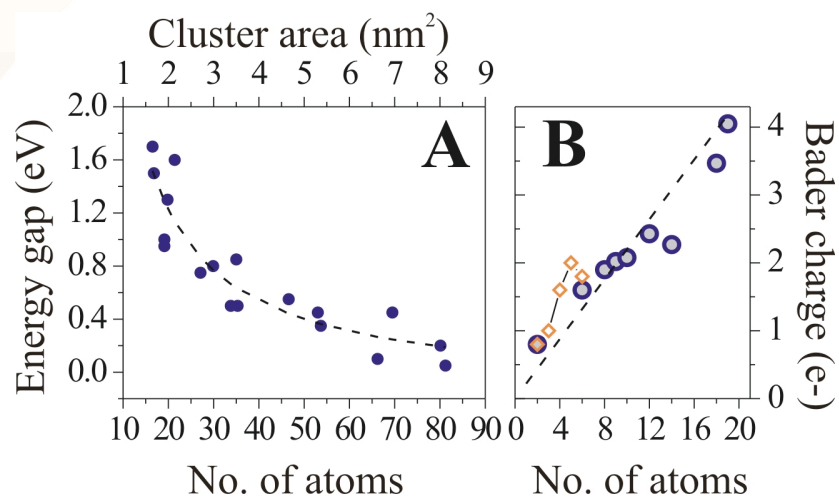
b) Au₁₈/MgO/Ag



Quantum dot behaviour



HOMO-LUMO gap closing (STM) and cluster charges (Bader analysis from DFT)



Ligand-protected gold clusters

Chemical: self-assembly/growth

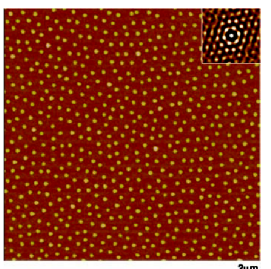


Fig. 1. AFM image of Au particles prepared by a micellar method (77) (z range, 20 nm). The inset shows the corresponding autocorrelation function indicating a high degree of hexagonal order. Analysis of the size distribution yields an average diameter of 7.9 ± 1.2 nm.

Boyen et al,
Science **297**, 1534 (2002)

-AuNPs on silicon oxide
(ligands removed)

Physical: deposition by soft-landing

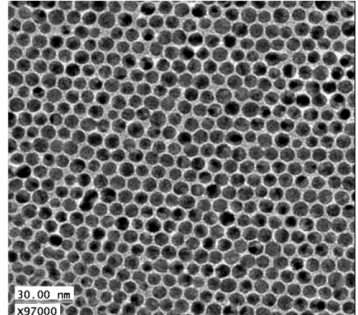


Figure 2. TEM image of C12S-AnII (core diameter 6.6 nm) film transferred at a surface pressure of 20 mN/m.

Liljeroth et al,
JACS **126**, 7126 (2004)

-2D compressed layer of
ligand-protected AuNPs

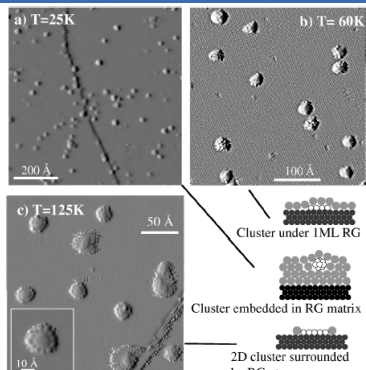


FIG. 1. Cluster-substrate morphology with the corresponding STM images for Ag₁₉/Kr/Pt(111) at different annealing temperatures. Also given are cartoons illustrating the proposed morphologies.

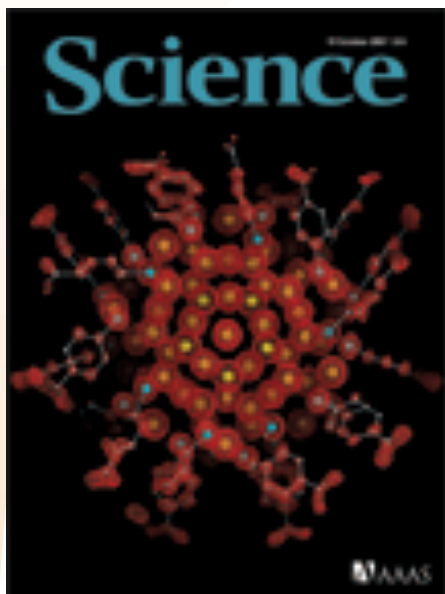
Schaub et al, PRL **86** (2001)

-Soft-landing of mass-selected
Ag₁₉ clusters on Kr/Pt(111)

UNIVERSITY OF JYVÄSKYLÄ

Nanoscience Center

Science 19 October 2007 – The first total-structure-determination of a thiolate-protected Au cluster (single-crystal Xray experiment)



Structure of a Thiol Monolayer–Protected Gold Nanoparticle at 1.1 Å Resolution

Pablo D. Jadzinsky,^{1,2*} Guillermo Calero,^{1*} Christopher J. Ackerson,^{1†} David A. Bushnell,¹ Roger D. Kornberg^{1‡}

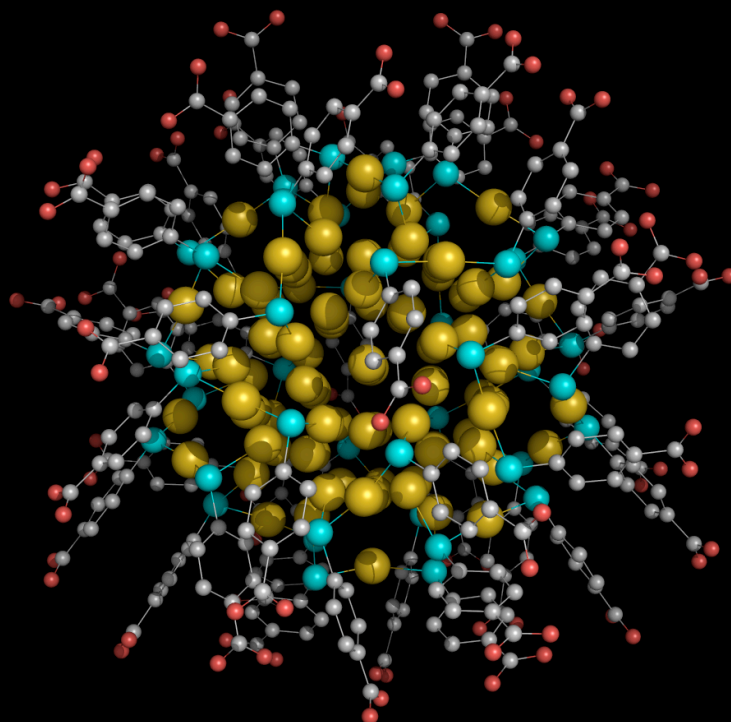
CHEMISTRY

Nano-Golden Order

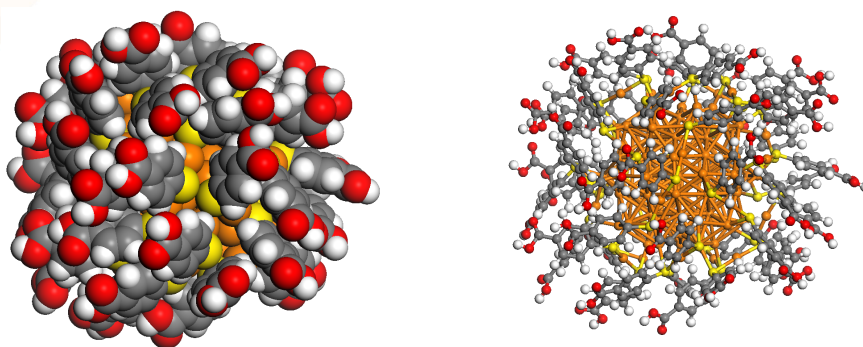
Robert L. Whetten and Ryan C. Price

An experimental tour de force reveals the crystal structure of a gold-thiolate nanocrystal compound and the surprising nature of the gold-sulfur bonding.

The proposed cover of Science 19 Oct 2007
(courtesy Roger Kornberg)

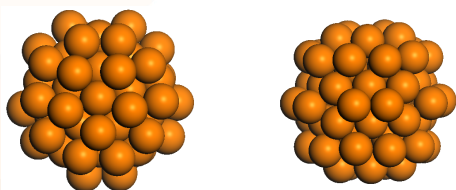


Anatomy of the Stanford cluster I:
 $\text{Au}_{102}(\text{p-MBA})_{44}$, Two visualizations
 (p-MBA = para-mercapto benzoic acid)

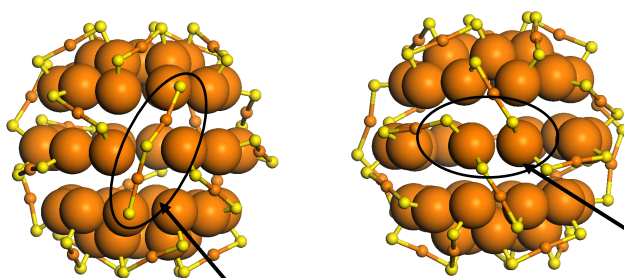


Initial coordinates: Jadzinsky et al Science Oct 19, 2007
 - necessary H added & CH bonds and COOH groups relaxed
 Full complex: 762 atoms and 3366 valence electrons
 (Walter et al, PNAS 2008)

Anatomy of the Stanford cluster II: core – shell !



Two views of the (D_{5h}, within 0.4 Å)
 Au_{79} core

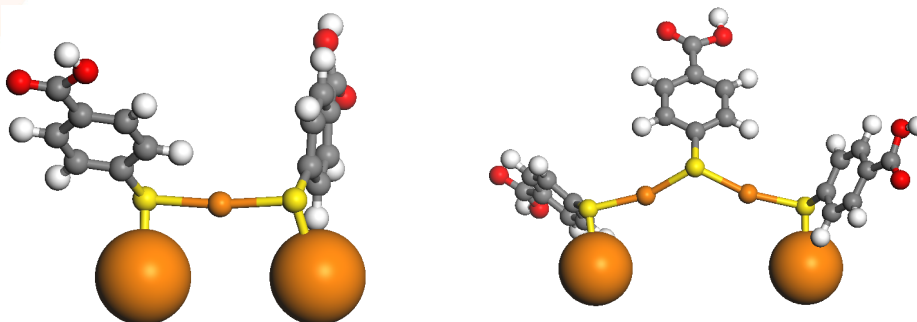
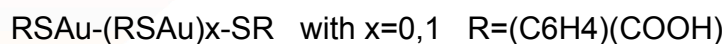


40-atom surface of the core
 +
 21 $\text{RSAu}-(\text{RSAu})_x\text{-SR}$ units
 (x=0 for 19 units and
 x=1 for 2 units)

2 Au(core) atoms with 2 SAu
 bonds each

long unit, x=1

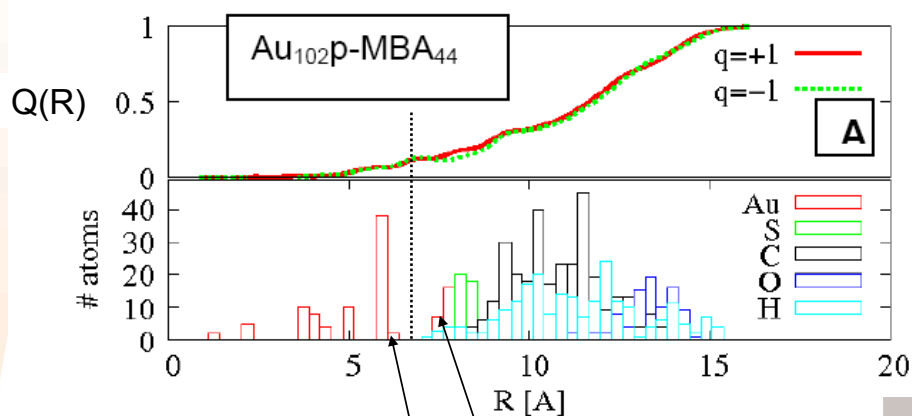
Anatomy of the Stanford cluster III: The two types of ligands



Anatomy of the Stanford cluster IV : A **metallic, electronically inert** Au₇₉ core

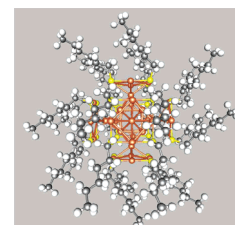
Radial analysis of charge re-distribution upon ionizing:

virtually no changes inside 5Å radius, 10 % of the charge at the surface of Au₇₉,
90% charging inside the Au₂₃(p-MBA)₄₄ protective layer

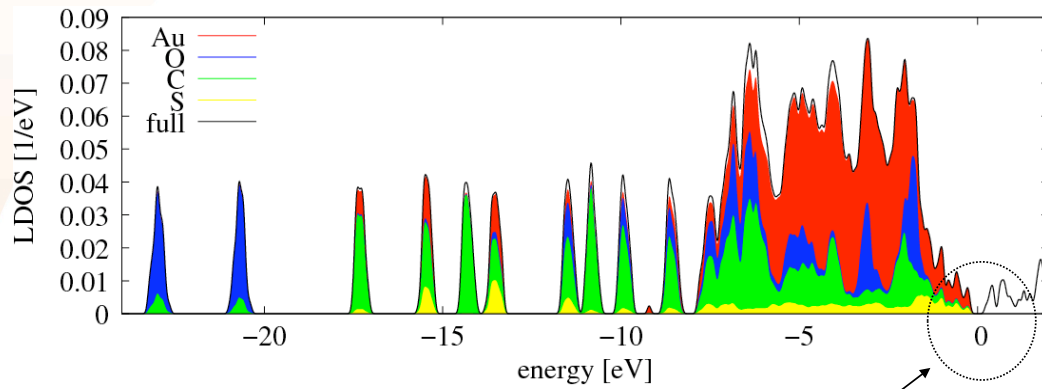


Surface layer (40 atoms) of the Au₇₉ core

Note: 23 Au atoms in the protective layer (cf. "Divide and Protect" model for Au₃₈(SR)₂₄ = Au₁₄(Au₄SR₄)₆ Häkkinen, Walter, Grönbeck, JPCB 110, 9927 2006))



The EDOS of Au102(pMBA)44



region of interest

(Global) angular momentum analysis of
Au(6s6p)-derived "conduction electron" states in the gold core

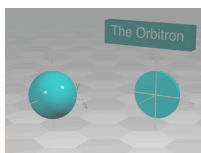
$$c_{i,l}(R_0) = \sum_m \int_0^{R_0} r^2 dr |\varphi_{i,lm}(r)|^2$$

$$\varphi_{i,lm}(r) = \int d\hat{r} Y_{lm}^*(\hat{r}) \psi_i(\vec{r})$$

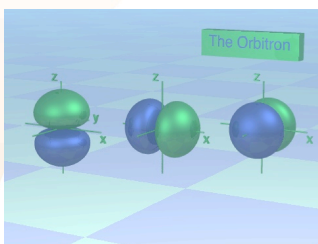
Evaluate the coefficients $c(R_0)$ for each
Kohn-Sham state i (done up to $\tilde{l} = 6$)

Atomic orbitals

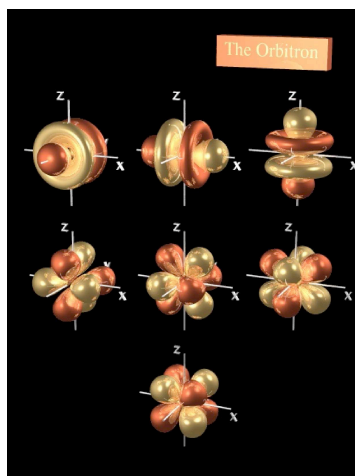
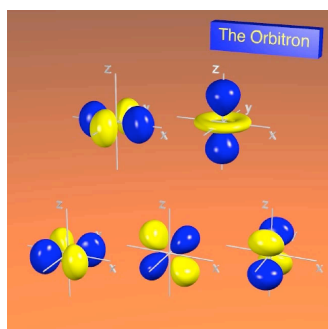
1s



2p

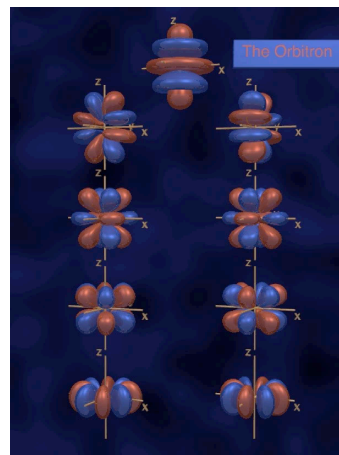


3d



4f

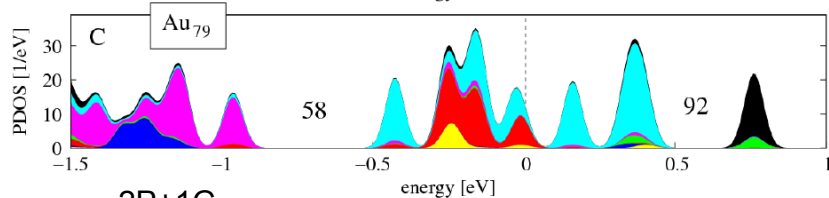
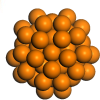
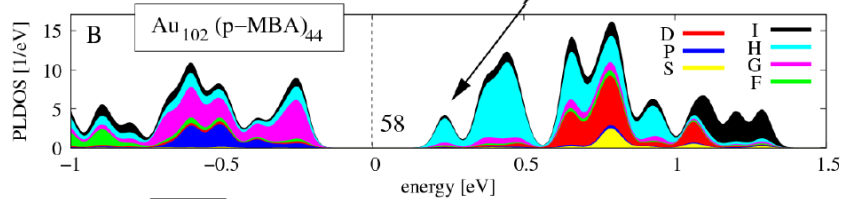
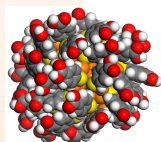
5g



<http://winter.group.shef.ac.uk/orbitron/>

Electronic structure: Angular momentum projected DOS around Fermi level (at E=0)

- Au₇₉ core supports the (expected) shell structure (58, 92 e gaps, proper symmetries)
- Upon dressing the core with 21 (RSAu-(RSAu)_x-SR) units, 21 conduction electrons depleted from the 3S+2D+1H manifold (→ surface-covalent S-Au(core) bonds), thereby revealing the **58 e gap**, which becomes the HOMO-LUMO gap of the protected cluster !!



2P+1G

3S+2D+1H

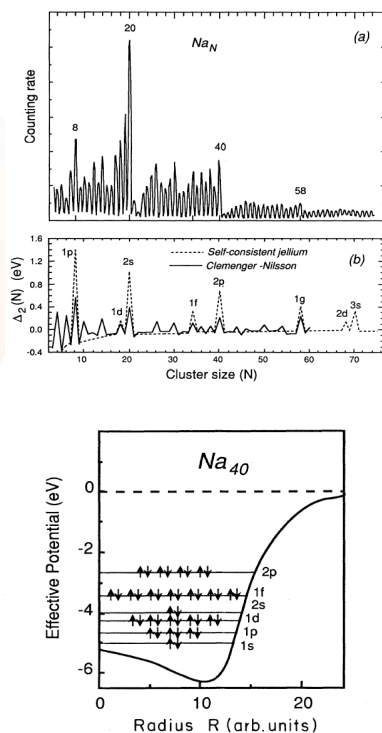


FIG. 3. Self-consistent effective potential of jellium sphere corresponding to Na_{40} with the electron occupation of the energy levels. After Chou *et al.*, 1984.

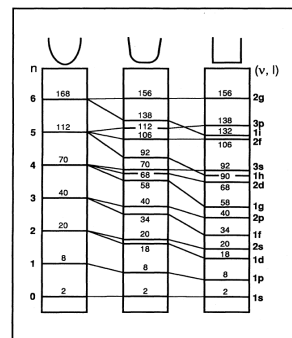
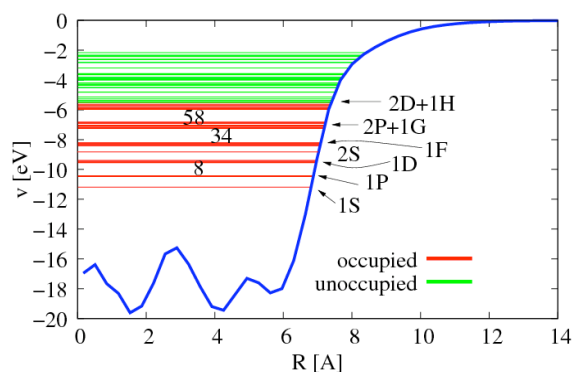


FIG. 2. Energy-level occupations for spherical three-dimensional, harmonic, intermediate, and square-well potentials. After Mayer and Jensen, 1955.



Au79 KS levels and effective radial potential 6s-only calculation (M. Walter)

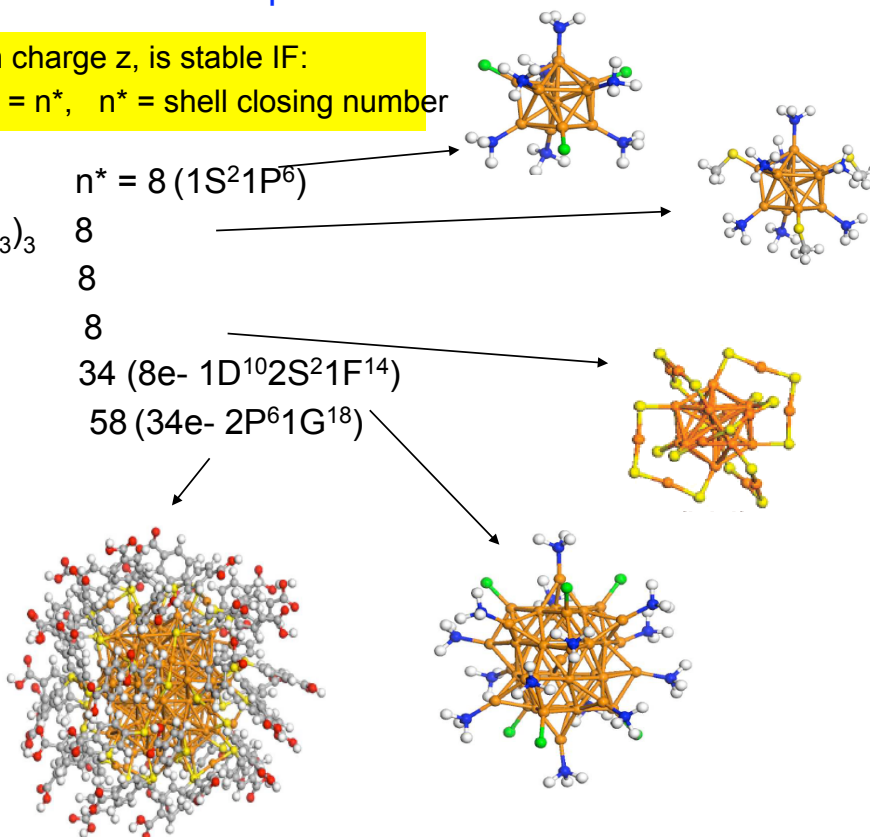
X-ray structures follow the simple rule:

($\text{L}_s \bullet \text{Au}_N \text{X}_M$) with charge z , is stable IF:
 $N(\text{Au}, 6s) - M - z = n^*$, $n^* = \text{shell closing number}$

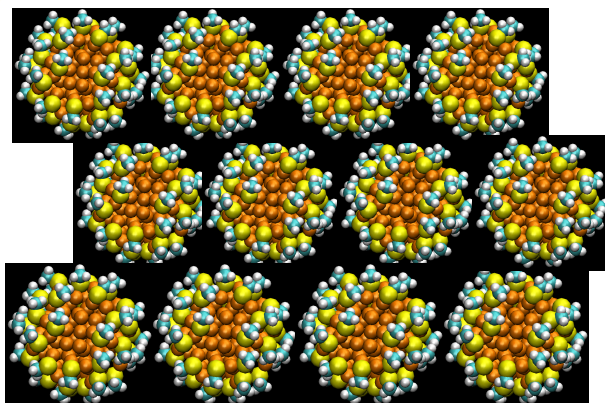
$\text{Au}_{11}(\text{PH}_3)_7\text{Cl}_3$	$n^* = 8 (1\text{S}^2 1\text{P}^6)$
$\text{Au}_{11}(\text{PH}_3)_7(\text{SCH}_3)_3$	8
$\text{Au}_{13}(\text{PH}_3)_{10}\text{Cl}_2^{3+}$	8
$\text{Au}_{25}(\text{SR})_{18}^-$	8
$\text{Au}_{39}(\text{PH}_3)_{14}\text{Cl}_6^-$	34 ($8e- 1\text{D}^{10} 2\text{S}^{21} 1\text{F}^{14}$)
$\text{Au}_{102}(\text{SR})_{44}$	58 ($34e- 2\text{P}^6 1\text{G}^{18}$)

Here $\text{L} = \text{PR}_3$
 and $\text{X} = \text{Cl}, \text{SR}$

L "weak ligand"
 X electron withdrawing
 (localizing) ligand

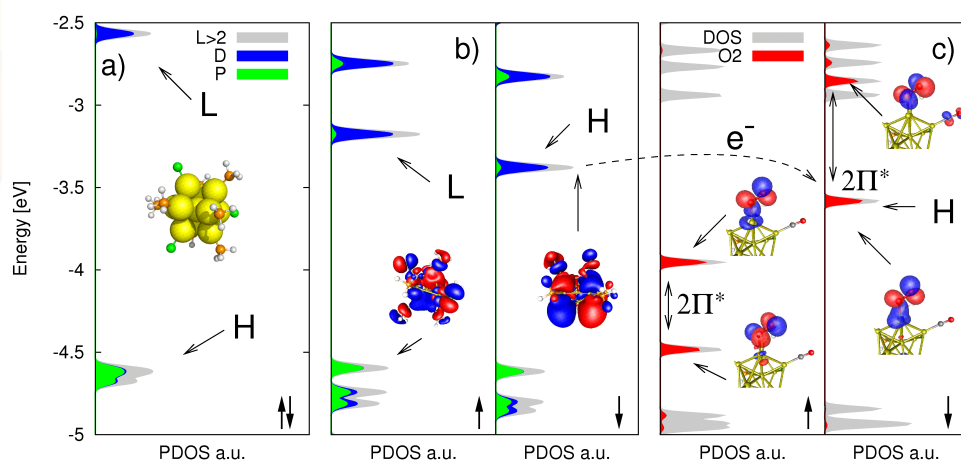


Robust (?) nanocatalysts – theorist's dream



Model catalyst : partially protected
 $\text{Au}_{11}(\text{PH}_3)_6\text{Cl}_2$

Activation of O₂ to superoxo O₂⁻



■ Animation